Astron. Astrophys. 317, 178–184 (1997)

ASTRONOMY
AND
ASTROPHYSICS

Abundance anomalies in main sequence A stars*

III. Nitrogen and sulphur

Inga Rentzsch-Holm

Institut für Astronomie und Astrophysik, Universität Kiel, D-24098 Kiel, Germany

Received 28 March 1996 / Accepted 3 May 1996

Abstract. Nitrogen and sulphur abundances in 15 sharp-lined 'normal' main sequence A stars are determined from new high-resolution CCD spectra. Non-LTE effects are taken into account.

Nitrogen abundances are distributed over an interval of 0.5 dex around the solar value of 8.05. Non-LTE abundance corrections range from -0.2 to -1.2 dex.

Sulphur is overabundant with respect to the sun by 0.1 to 0.6 dex in all program stars. Taking non-LTE effects into account reduces the overabundances, but cannot remove them entirely; non-LTE abundance corrections $\Delta \log \epsilon$ are typically -0.1 dex.

Comparison with previously derived carbon abundances reveals that carbon and nitrogen behave very similarly in each star. Thus the anticorrelation of [C/Si] with [Si/H] found by Holweger (1992) is also true for [N/Si]. For sulphur a similar anticorrelation is also possible.

Key words: stars: abundances – stars: early-type – stars: individual: Sirius

1. Introduction

This work is closely connected to the two papers by Lemke (1989, 1990) dealing with the chemical composition of 16 bright, sharp-lined normal main-sequence A stars. Lemke's work reveals a wide spread in abundance patterns for these stars that is contrary to their 'normal' classification. The Ti/Fe and Si/Fe ratios are solar while the Ba/Fe and Sr/Fe ratios vary from star to star. Both elements are typically enhanced by 1.0 dex relative to the sun. Calcium and carbon on the other hand show a scatter of one order of magnitude.

Subsequent work on the same stars by Holweger (1992) and Holweger & Stürenburg (1993) reveals a tight anticorrelation between carbon and silicon which was interpreted as a signature of gas-dust separation in the protostellar or circumstellar environment. Volatile elements like C, N, O remain in the gas phase, hence stars with a large C/Si ratio have preferentially accreted gas. Accretion of dust on the other hand leads to a small C/Si ratio, because refractory elements like silicon and iron have condensed onto dust grains. In addition diffusion processes in the atmosphere partly contaminate the chemical composition obtained by differential accretion of gas or dust.

Recently this picture has been elaborated further (Holweger et al. 1995): while for the metal-poor λ Bootis stars the accretion model still holds true, it fails for the 'normal' A stars. The abundance patterns of the latter reveal clear signatures of diffusion. According to theoretical calculations of radiative acceleration (Michaud et al. 1976, Gonzalez et al. 1995), in A stars carbon and nitrogen should settle, because at the bottom of the convection zone their radiative acceleration outwards is smaller than the gravity acceleration inwards.

The aim of this paper is to investigate a possible correlation between carbon and nitrogen abundances in the 'normal' A stars in order to support or reject the above models of chemical separation in these stars. Newly CCD spectra of these stars are therefore analyzed to obtain reliable non-LTE abundances of nitrogen. Lines of sulphur and iron in the same spectral range are analyzed as well. The derived abundances are discussed in the context of earlier work.

2. Observations

High-resolution spectra were recorded with the Coudé spectrograph (CES) of the ESO 1.4 m telescope during two observing runs in 1993 and 1994 (Table 1). They were taken with the short camera equipped with ESO CCD #9 (RCA SID 503, 1024×640 pixels) and cover a 70-Å wide spectral band centred at 8665 Å.

The spectrum of a nearby O star was recorded after each programme star to facilitate flatfield correction. The severe interference fringes which show up in the infrared spectral region could be almost totally eliminated in this way.

The very sharp-lined A1V star HR 4138 was used for wavelength calibration. Normalization of the spectra at this point of the data reduction is impossible, because the strong lines of the Paschen series of hydrogen inhibit a correct continuum placement.

* Based on observations obtained at the European Southern Observatory, La Silla, Chile

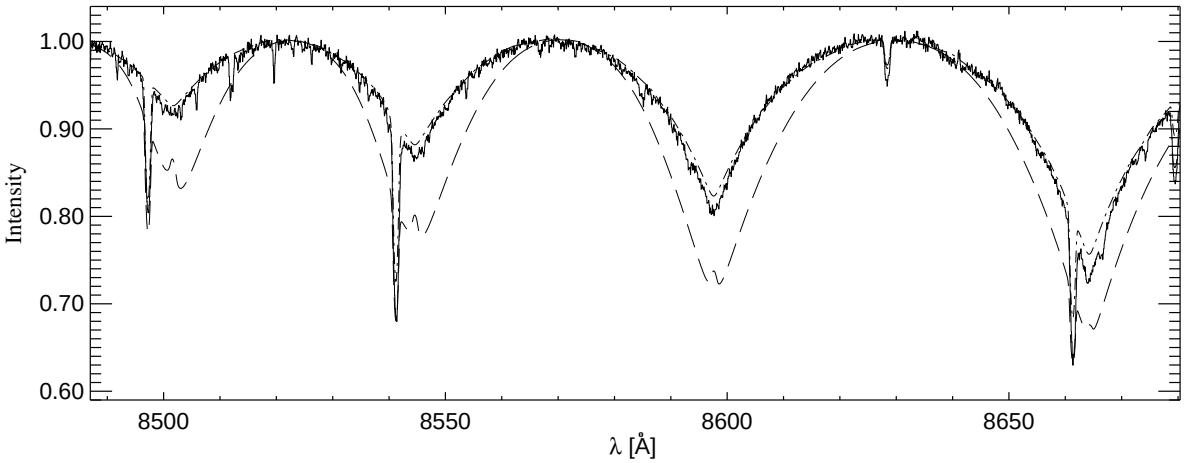

Fig. 1. Infrared spectrum of Vega. Solid line: observed spectrum (Babel, private communication). Dashed line: synthetic spectrum calculated with an ATLAS9 (9500, 3.90, -0.5) model atmosphere, theory of ATLAS9 for the Paschen lines. Dashed-dotted line: similar synthetic spectrum but using VCS tables for the Paschen lines. All spectra are normalized to 1.0

Table 1. Stellar parameters of the program stars (Lemke 1989)

HR	Name	Sp.Type	$T_{\rm eff}$	$\log g$	$\xi_{\rm micro}$	$v \cdot \sin i$
1448		A2Vs	9200	3.70	3.0	24
1975		A0Vs	10170	4.50	1.3	33
2491	Sirius	A1Vm	9900	4.30	2.0	16
3136		A1V	9650	4.00	3.0	≤ 41
3383		A1V	9770	4.00	2.5	4.5
3963		A0V	10900	3.65	1.3	28
4138		A1V	9300	3.65	3.0	6.5
4359	θ Leo	A2V	9460	3.45	2.0	21
5798		A0V	9900	3.70	2.5	38
6070		A0V	9600	4.50	2.8	36
6548	53 Oph	A2V	9500	3.90	2.0	27
7610	ϕ Aql	A1IV	9540	4.30	2.0	25
7773	ν Cap	B9.5V	10300	3.80	1.2	22
7883	ι Del	A2V	9100	4.30	3.0	37
8576	β PsA	A0V	9600	4.20	2.0	26

3. Model atmospheres and spectrum synthesis

ATLAS9 model atmospheres (Kurucz 1992) are calculated using the stellar parameters and element compositions derived by Lemke (1989, 1990). The stars and their adopted parameters are listed in Table 1. The differences between the new models and those based on ATLAS6 (Kurucz 1979) are insignificant.

4. Paschen lines of hydrogen

The infrared spectral region is distorted by strong lines of the hydrogen Paschen series. A spectrum of Vega (Babel, private communication) recorded at OHP with the Aurélie spectrograph (Gillet et al. 1994) at a resolution of 30 000 covers the four Paschen lines P13 to P16. It allows a detailed comparison to be made with calculated line profiles.

In an earlier work (Rentzsch-Holm 1996) the opacity of the Paschen lines was calculated using the theory implemented in ATLAS9 (Kurucz 1970). This theory is valid only for the wings of high-series members and should not be used to calculate detailed line profiles for comparison with observation. A comparison of the synthetic spectrum computed with an ATLAS9 model atmosphere (9500, 3.90, -0.5) with the observed spectrum (Fig. 1) shows that the theoretical profiles (dashed line) are too strong.

The 'unified theory' of line broadening generates normalized Stark profiles for hydrogen lines (Vidal et al. 1970, 1971). Using their program (Vidal et al. 1973) Lemke calculated tables (analogous to the VCS tables of the Balmer lines) for the first 17 Paschen lines of hydrogen covering electron densities from 10^{10} to 10^{18} cm^{-3} and temperatures between 2500 and 80000 K. A synthetic spectrum computed by linearly interpolation in those tables fits the observational data (Fig. 1, dashed-dotted line) adequately. The remaining differences in the line cores vanish if the gravity is reduced by 0.10 dex.

A detailed comparison between the profiles of Vidal et al. (1973), and the recently calculated Stark profiles of Stehlé (1994) using the Model Microfield Method, reveals significant differences in the line cores which diminish or disappear when Doppler broadening dominates (Clausset et al. 1994). Profiles for the higher members of the Paschen series have not yet been given in the literature.

To synthesize P12 and P13 the Paschen lines needed in this work, Stark profiles are taken from the tables of Lemke. For all program stars synthetic spectra are computed assuming solar nitrogen and sulphur abundances, 8.05 (Rentzsch-Holm 1996) and 7.21 (Anders & Grevesse 1989) respectively. The observed spectra are then normalized to the synthetic ones to obtain the correct continuum placement, as shown in Fig. 2.

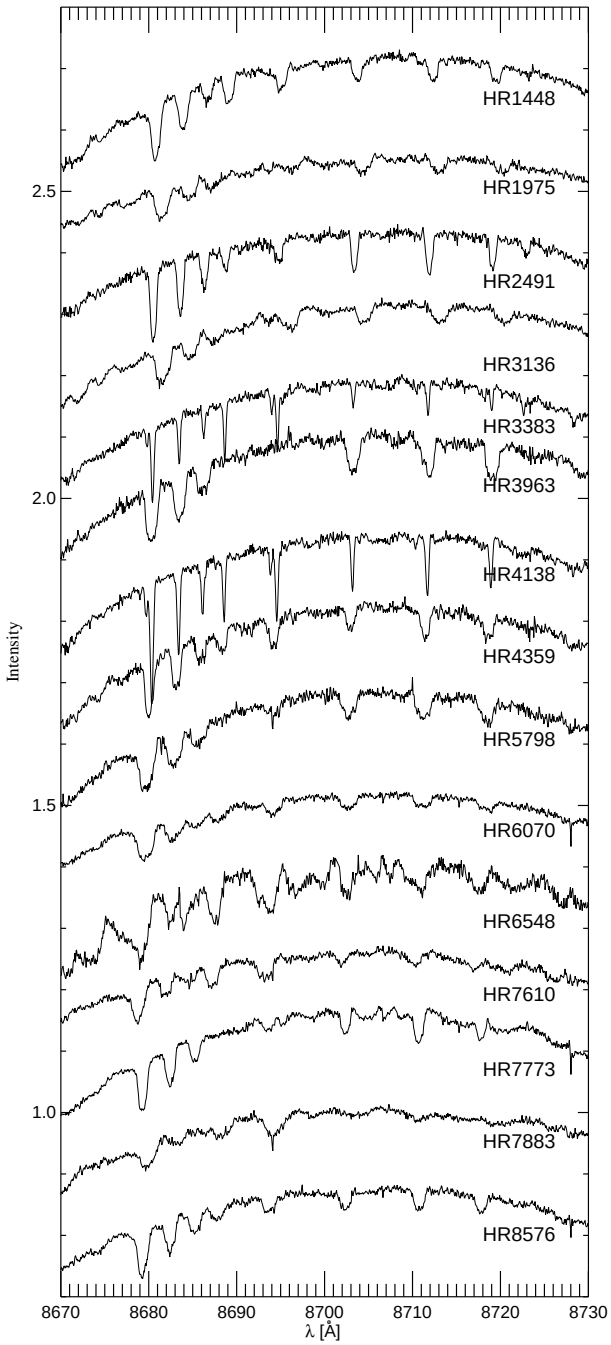

Fig. 2. Observed spectra of all stars listed in Table 1; spectra are shifted upward by 13 % with respect to the preceeding one and normalized to the theoretically calculated wings of the Paschen lines P12 and P13

5. Abundance analysis

Data for the lines used in this analysis are taken from the tables of Wiese et al. (1966) and correspond closely to the line lists of Sadakane & Okyudo (1989) (hereafter SO) and Takada-Hidai & Takeda (1995) (hereafter THT). The f-values for nitrogen are derived from the Opacity Project data base provided by the CDS Strasbourg (Cunto et al. 1993, Seaton 1992, hereafter OP). For sulphur and iron the transition probabilities are taken from Wiese et al. (1966) and Fuhr et al. (1988), respectively.

Equivalent widths for all detectable lines in the programme stars are given in Table 2. The nitrogen $\lambda\lambda$8680.26 line is blended with sulphur $\lambda\lambda$8680.46 and the equivalent width given refers to the entire blend. For spectrum synthesis the sulphur abundance for this line is assumed to be the same as that corresponding to the $\lambda\lambda$8694 blend. Owing to rotational broadening the $\lambda\lambda$8694 blend cannot be resolved into single components – except in the case of the two very sharp-lined stars HR 3383 and HR 4138, where the equivalent width of the components are given in brackets. Otherwise the table gives the equivalent width of the blend.

Unfortunately the spectrum of HR 6548 is heavily distorted by some remaining fringes. The three nitrogen lines $\lambda\lambda$8683.40, 8703.26 and 8718.84 give only an upper limit of $\log \epsilon_{\rm N}$.

In HR 7883 the spectral range above $\lambda\lambda$8700 is also heavily distorted by fringes. The $\lambda\lambda$8686.16 line gives only an upper limit of the nitrogen abundance.

The iron line in HR 7773 is hardly detectable, so the iron abundance given is an upper limit.

5.1. Nitrogen

Detailed non-LTE calculations are performed for each model atmosphere using the Kiel non-LTE code of Steenbock & Holweger (1984) and the nitrogen model atom described by Rentzsch-Holm (1996).

As already mentioned by THT the non-LTE abundance corrections ($\Delta \log \epsilon = \log \epsilon_{\rm NLTE} - \log \epsilon_{\rm LTE}$) depend markedly on effective temperature; in the parameter range investigated in this work ($8800 < {\rm T_{eff}} < 10900$) $\Delta \log \epsilon$ increases with $\rm T_{eff}$. Two other processes should not be neglected. First, a higher gravity generally leads to higher collisional rates and hence reduces the non-LTE effects. Secondly, in the special case of nitrogen the carbon abundance plays an important role in non-LTE calculations (Rentzsch-Holm 1996), because it strongly affects the resonance lines of nitrogen via bound-free continua in the UV. A higher carbon abundance leads to smaller non-LTE abundance corrections.

However, the abundance corrections derived in this work are not representative of truly photospheric N I lines. Owing to the presence of the Paschen lines the nitrogen lines form higher in the atmosphere where departures from LTE are generally larger. A clear trend to larger non-LTE abundance corrections towards the line core of P13 is visible from Table 2, reflecting the decreasing depth of line formation.

For all program stars the non-LTE abundances from the individual lines reveal a significantly smaller scatter than when LTE is employed.

5.2. Sulphur

Where a determination of the equivalent width of the $\lambda\lambda$8694 blend is possible, sulphur shows significant overabundances with respect to the Sun.

Table 2. Nitrogen abundances (LTE and NLTE) and non-LTE abundance corrections ($\Delta \log \epsilon = \log \epsilon_{\rm NLTE} - \log \epsilon_{\rm LTE}$) derived from individual photospheric lines. Transition probabilities for nitrogen, sulphur and iron are taken from OP, Wiese et al. (1966) and Fuhr et al. (1988) respectively. Equivalent width are given in mÅ

			HR 1448				HR 1975				HR 2491			
Ion	λ [Å]	$\log gf$	W_λ	$\log\epsilon_{\rm LTE}$	$\log\epsilon_{\rm NLTE}$	$\Delta\log\epsilon$	W_λ	$\log\epsilon_{\rm LTE}$	$\log\epsilon_{\rm NLTE}$	$\Delta\log\epsilon$	W_λ	$\log\epsilon_{\rm LTE}$	$\log\epsilon_{\rm NLTE}$	$\Delta\log\epsilon$
N I	8680.26	+0.228	117	8.55	7.95	-0.60	93	8.73	8.07	-0.66	111	8.85	7.95	-0.90
S I	8680.46	−0.23												
N I	8683.40	−0.051	74	8.34	7.94	-0.40	46	8.25	7.89	-0.36	75	8.62	7.99	-0.63
	8686.16	−0.453	31	8.05	7.82	-0.23	34	8.39	8.10	-0.29	51	8.61	8.13	-0.48
Fe I	8688.64	−1.212	52	8.00	–	–	–	–	–	–	31	8.15	–	–
S I	8693.24	−1.38												
	8693.98	−0.52	50	7.47	7.33	-0.14	25	7.54	7.46	-0.08	41	7.69	7.59	-0.10
	8694.70	+0.05												
N I	8703.26	−0.453	43	8.14	7.91	-0.23	39	8.40	8.12	-0.28	52	8.51	8.09	-0.42
	8711.71	−0.346	41	8.00	7.78	-0.22	41	8.33	8.04	-0.29	59	8.51	8.07	-0.44
	8718.84	−0.419	32	7.96	7.76	-0.20	25	8.13	7.89	-0.24	39	8.30	7.92	-0.38

			HR 3136				HR 3383				HR 3963			
Ion	λ [Å]	$\log gf$	W_λ	$\log\epsilon_{\rm LTE}$	$\log\epsilon_{\rm NLTE}$	$\Delta\log\epsilon$	W_λ	$\log\epsilon_{\rm LTE}$	$\log\epsilon_{\rm NLTE}$	$\Delta\log\epsilon$	W_λ	$\log\epsilon_{\rm LTE}$	$\log\epsilon_{\rm NLTE}$	$\Delta\log\epsilon$
N I	8680.26	+0.228	105	8.55	7.72	-0.83	59	7.89	7.35	-0.54	128	9.43	8.20	-1.23
S I	8680.46	−0.23												
N I	8683.40	−0.051	61	8.27	7.72	-0.55	29	7.79	7.38	-0.41	99	9.14	8.24	-0.90
	8686.16	−0.453	35	8.09	7.68	-0.41	19	7.93	7.56	-0.37	62	8.85	8.27	-0.58
Fe I	8688.64	−1.212	23	7.87	–	–	33	8.12	–	–	–	–	–	–
S I	8693.24	−1.38												
	8693.98	−0.52	53	7.73	7.61	-0.12	(12)49	7.75	7.64	-0.11	–	–	–	–
	8694.70	+0.05					(33)							
N I	8703.26	−0.453	47	8.30	7.90	-0.40	14	7.66	7.36	-0.30	82	8.97	8.40	-0.57
	8711.71	−0.346	53	8.29	7.86	-0.43	19	7.71	7.39	-0.32	88	8.96	8.34	-0.62
	8718.84	−0.419	30	8.05	7.65	-0.40	10	7.54	7.21	-0.33	84	9.03	8.40	-0.63

			HR 4138				HR 4359				HR 5798			
Ion	λ [Å]	$\log gf$	W_λ	$\log\epsilon_{\rm LTE}$	$\log\epsilon_{\rm NLTE}$	$\Delta\log\epsilon$	W_λ	$\log\epsilon_{\rm LTE}$	$\log\epsilon_{\rm NLTE}$	$\Delta\log\epsilon$	W_λ	$\log\epsilon_{\rm LTE}$	$\log\epsilon_{\rm NLTE}$	$\Delta\log\epsilon$
N I	8680.26	+0.228	105	8.33	7.77	-0.56	109	8.54	7.82	-0.72	150	9.26	8.29	-0.97
S I	8680.46	−0.23												
N I	8683.40	−0.051	63	8.19	7.81	-0.38	81	8.49	7.94	-0.55	112	8.99	8.33	-0.66
	8686.16	−0.453	40	8.22	7.93	-0.29	45	8.30	7.94	-0.36	78	8.82	8.42	-0.40
Fe I	8688.64	−1.212	42	7.93	–	–	44	8.23	–	–	26	8.17	–	–
S I	8693.24	−1.38												
	8693.98	−0.52	(19)77	7.80	7.65	-0.15	64	7.83	7.69	-0.14	51	7.90	7.80	-0.10
	8694.70	+0.05	(54)											
N I	8703.26	−0.453	34	8.00	7.80	-0.20	42	8.13	7.84	-0.29	74	8.64	8.30	-0.34
	8711.71	−0.346	44	8.05	7.80	-0.25	60	8.27	7.94	-0.33	83	8.66	8.28	-0.38
	8718.84	−0.419	29	7.92	7.68	-0.24	52	8.27	7.94	-0.33	72	8.62	8.26	-0.36

			HR 6070				HR 6548				HR 7610			
Ion	λ [Å]	$\log gf$	W_λ	$\log\epsilon_{\rm LTE}$	$\log\epsilon_{\rm NLTE}$	$\Delta\log\epsilon$	W_λ	$\log\epsilon_{\rm LTE}$	$\log\epsilon_{\rm NLTE}$	$\Delta\log\epsilon$	W_λ	$\log\epsilon_{\rm LTE}$	$\log\epsilon_{\rm NLTE}$	$\Delta\log\epsilon$
N I	8680.26	+0.228	118	8.79	8.24	-0.55	–	–	–	–	93	8.40	7.86	-0.54
S I	8680.46	−0.23												
N I	8683.40	−0.051	70	8.46	8.14	-0.32	<58	<8.26	<7.88	-0.38	38	8.00	7.68	-0.32
	8686.16	−0.453	43	8.43	8.21	-0.22	–	–	–	–	23	8.04	7.81	-0.23
Fe I	8688.64	−1.212	38	7.98	–	–	–	–	–	–	49	8.21	–	–
S I	8693.24	−1.38												
	8693.98	−0.52	40	7.43	7.31	-0.12	–	–	–	–	68	7.78	7.65	-0.13
	8694.70	+0.05												
N I	8703.26	−0.453	39	8.29	8.11	-0.18	<77	<8.72	<8.37	-0.35	27	8.05	7.84	-0.21
	8711.71	−0.346	32	8.08	7.90	-0.18	–	–	–	–	32	8.05	7.82	-0.23
	8718.84	−0.419	26	8.06	7.89	-0.17	<61	<8.52	<8.21	-0.31	31	8.12	7.91	-0.21

Table 2. continued

			HR 7773				HR 7883				HR 8576			
Ion	λ [Å]	$\log gf$	W_λ	$\log\epsilon_{\rm LTE}$	$\log\epsilon_{\rm NLTE}$	$\Delta\log\epsilon$	W_λ	$\log\epsilon_{\rm LTE}$	$\log\epsilon_{\rm NLTE}$	$\Delta\log\epsilon$	W_λ	$\log\epsilon_{\rm LTE}$	$\log\epsilon_{\rm NLTE}$	$\Delta\log\epsilon$
N I	8680.26	+0.228	107	8.97	7.90	-1.07	86	8.09	7.74	-0.35	126	9.00	8.28	-0.72
S I	8680.46	−0.23												
N I	8683.40	−0.051	76	8.69	7.94	-0.75	34	7.85	7.62	-0.23	80	8.64	8.21	-0.43
	8686.16	−0.453	47	8.54	8.01	-0.53	<18	<7.87	<7.68	-0.19	53	8.59	8.29	-0.30
Fe I	8688.64	−1.212	<17	<8.15	–	–	48	7.73	–	–	39	8.10	–	–
S I	8693.24	−1.38												
	8693.98	−0.52	24	7.67	7.59	-0.08	80	7.57	7.41	-0.16	44	7.56	7.44	-0.12
	8694.70	+0.05												
N I	8703.26	−0.453	47	8.39	7.95	-0.44	–	–	–	–	48	8.41	8.17	-0.24
	8711.71	−0.346	67	8.60	8.06	-0.54	–	–	–	–	46	8.27	8.04	-0.23
	8718.84	−0.419	42	8.31	7.88	-0.43	–	–	–	–	37	8.21	8.01	-0.20

Non-LTE effects for sulphur are taken into account by interpolating for $T_{\rm eff}$ and $\log W_\lambda$ in the tables of THT for the two lines $\lambda\lambda$8693.98 and $\lambda\lambda$8694.70.

The resulting non-LTE abundance corrections are too small, $|\Delta\log\epsilon| < 0.2$ dex, to remove fully the general overabundance of sulphur. Only in HR 1448 and HR 6070 does $\log\epsilon_{\rm S}$ agree with the solar abundance within the error limits.

5.3. Iron

The LTE iron abundance derived from the $\lambda\lambda$8688.64 line is larger in all program stars than the LTE abundance derived in other spectral regions (Lemke 1989). The latter are expected to be more reliable, since they are based on a richer sample of lines.

Non-LTE effects in the infrared are expected to be larger than in the visible owing to the presence of the Paschen lines (see Sect. 5.1). For normal A stars, non-LTE abundance corrections of neutral iron are always positive (Rentzsch-Holm 1995). Hence, non-LTE cannot account for the discrepancy between the iron abundances in the two different spectral ranges.

6. Comparison with previous works

This work has one star in common with the analysis of THT, namely HR 7773 (ν Cap). The equivalent widths differ only by $\pm$16 %. When the same f-values are used, the present abundances agree with those of THT within 0.03 dex for nitrogen and 0.04 dex for sulphur.

SO give equivalent widths for HR 4359 (θ Leo) that are considerably larger in the wings of the Paschen lines than those derived in this work. The resulting nitrogen abundance is 0.47 dex lower than the LTE abundance derived above for the 5 lines in common, if differences in f-values are taken into account. Using their equivalent width a difference of 0.30 dex still remains for nitrogen. A plausible explanation is that in their analysis SO neglected the strong continuum depression (3 – 20 %) caused by the Paschen lines. Test calculations show that the abundance derived in the present work, using f-values and equivalent width of SO, agrees completely with their abundance of $\log\epsilon_{\rm N}$ = 7.84 if the opacity of the Paschen lines is neglected in spectrum synthesis.

Table 3. Nitrogen and sulphur abundances for all program stars together with carbon, iron and silicon abundances from Holweger & Stürenburg (1993)

HR	[N/H]	$\Delta\log\epsilon_{\rm N}$	[S/H]	$\Delta\log\epsilon_{\rm S}$	[C/H]	[Fe/H]	[Si/H]
1448	-0.19	-0.31	0.12	-0.14	-0.11	0.24	-0.06
1975	-0.03	-0.35	0.25	-0.08	-0.23	0.11	0.28
2491	-0.02	-0.54	0.38	-0.10	-0.76	0.33	0.38
3136	-0.29	-0.50	0.40	-0.12	-0.77	0.35	0.17
3383	-0.67	-0.37	0.43	-0.11	-0.55	0.39	–
3963	0.26	-0.75	–	–	0.21	0.17	–
4138	-0.25	-0.32	0.44	-0.15	-0.02	0.23	-0.42
4359	-0.15	-0.43	0.48	-0.14	-0.16	0.43	0.15
5798	0.26	-0.52	0.59	-0.10	0.31	-0.08	-0.57
6070	0.03	-0.27	0.10	-0.12	-0.21	0.07	0.21
6548	0.10	-0.35	–	–	-0.20	0.30	–
7610	-0.23	-0.29	0.44	-0.13	-0.54	0.46	–
7773	-0.09	-0.62	0.38	-0.08	-0.26	0.08	0.21
7883	-0.37	-0.26	0.20	-0.16	-0.63	0.09	–
8576	0.12	-0.35	0.23	-0.12	-0.03	0.07	0.25
Sun	8.05	-0.05	7.21	–	8.58	7.51	7.55

7. Discussion

Table 3 presents the mean non-LTE abundances of nitrogen and sulphur derived in Sect. 5 together with their mean non-LTE abundance corrections. In addition the last three columns give the non-LTE abundances of carbon and iron and the LTE abundance of silicon taken from Holweger & Stürenburg (1993).

According to the accretion/diffusion model (see Sect. 1) nitrogen should behave like carbon. Both are volatile elements which remain in the gas phase during any gas-dust separation and diffusion causes both elements to settle. Since carbon is more abundant than nitrogen, saturation effects are stronger for the former.

Fig. 3 shows the anticorrelation of [C/Si] and [Si/H] (asterisks) found in Holweger & Stürenburg (1993) – this figure

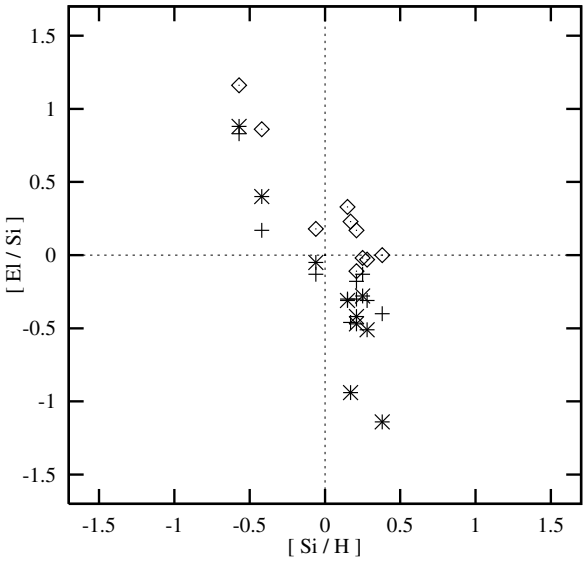

Fig. 3. [C/Si] (asterisks), [N/Si] (plus signs) and [S/Si] (diamonds) versus [Si/H]; carbon and silicon abundances from Holweger & Stürenburg (1993). Dotted lines indicate solar abundance ratios. Carbon and nitrogen reveal a tight anticorrelation

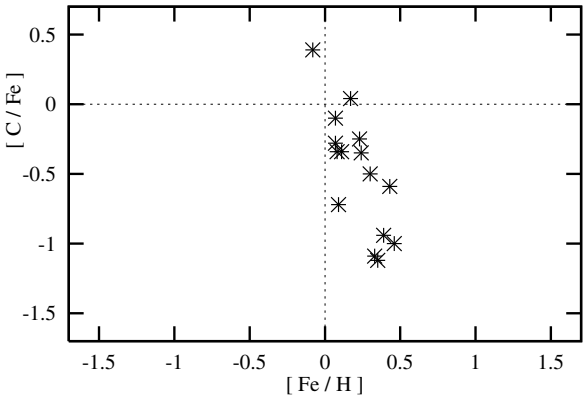

Fig. 4. [C/Fe] versus [Fe/H] for all program stars (Holweger & Stürenburg 1993). Dotted lines indicate solar abundance ratios

is comparable to their Fig. 2 without the λ Boo stars. Nitrogen and sulphur are now included in this figure (plus signs and diamonds respectively). The [N/Si] ratio follows the anticorrelation of [C/Si]. For all stars of the sample the [S/Si] ratio is larger than the respective [C/Si] and [N/Si] ratio. Nevertheless an anticorrelation similar to that found for carbon and nitrogen is possible.

For sulphur, and possibly also for carbon and nitrogen, the anticorrelation found above strongly depends on two stars, HR 5798 and HR 4138. Both spectra are free of residual fringes and should yield reliable abundances. The typical uncertainties from measuring the equivalent width are 0.1 dex and after non-LTE corrections are applied, the scatter in the individual lines is in most cases smaller than 0.1 dex. The reality of the observed anticorrelations, therefore seems to be confirmed.

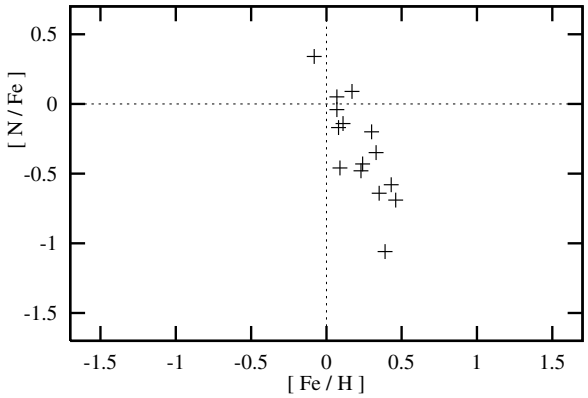

Fig. 5. [N/Fe] versus [Fe/H] for all program stars (iron abundance from Holweger & Stürenburg 1993). Dotted lines indicate solar abundance ratios

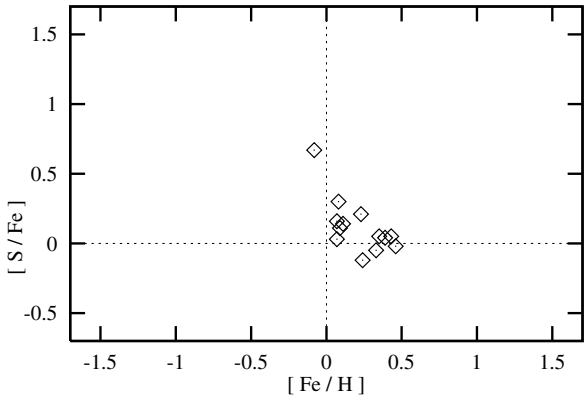

Fig. 6. [S/Fe] versus [Fe/H] for all program stars (iron abundance from Holweger & Stürenburg 1993). Dotted lines indicate solar abundance ratios

Table 3 shows that the silicon abundance for five of the 15 program stars could not be derived, but iron abundances exist for all of them. Since silicon and iron behave quite similarly in the gas/dust model, the [C/Fe] and [N/Fe] ratios should give trends similar to those seen in silicon and are thus available for the whole sample.

Figs. 4 and 5 show the respective ratios versus iron abundance. Since iron varies across only a small interval, -0.1 dex $<$ [Fe/H] $<$ 0.5 dex, the anticorrelation has a steeper gradient than in the case of silicon. But there is a clear correspondence between the two elements carbon and nitrogen.

The [S/Fe] ratio is larger than the solar one in most program stars. In view of the uncertainties in the abundance determination there is no clear correlation visible in the data (Fig. 6). However an anticorrelation as found above for [C/Fe] and [N/Fe] cannot be excluded.

An extensive search for other correlations reveals (apart from a non-systematic scatter) no obvious dependence on effective temperature or gravity, that is evolutionary effects are small or absent.

Acknowledgements. The author expresses her gratitude to H. Holweger for suggesting this work and for numerous discussions. Thanks are also due to M. Lemke for making the VCS tables available and to T. Rauch for helping with the computations. The author is grateful to H. Holweger for providing the ESO spectra and to J. Babel for providing an unpublished infrared spectrum of Vega. Support from a graduate student fellowship from Schleswig-Holstein is also acknowledged.

References

Anders, E., Grevesse, N. 1989, Geochim. Cosmochim. Acta. 53, 197
Clausset, F., Stehlé, C., Artru, M.-C. 1994, A&A 287, 666
Cunto, W., Mendoza, C., Ochsenbein, F., Zeippen, C.J. 1993, Bull. Inform. CDS 42, p. 39
Fuhr, J.R., Martin, G.A., Wiese, W.L. 1988, Atomic Transition Probabilities, Iron through Nickel. J. Phys. Chem. Ref. Data Vol.17, Suppl. No. 4
Gillet, D., Burnage, R., Kohler, D., Lacroix, D., Adrianzyk, G., Baietto, J.C., Berger, J.P., Goillandeau, M., Guillaume, C., Joly, C., Meunier, J.P., Rimbaud, G., Vin, A. 1994, A&AS 108, 181
Gonzalez, J.-F., Artru, M.-C., Michaud, G. 1995, A&A 302, 788
Holweger, H. 1992, in The Atmospheres of Early-Type Stars, Lecture Notes in Physics Vol. 401, eds. U. Heber and C.S. Jeffery, p. 48
Holweger, H., Stürenburg, S. 1993, in Peculiar Versus Normal Phenomena in A-Type and Related Stars, ASP Conference Series, Vol. 44, eds. M.M. Dworetsky, F. Castelli and R. Faraggiana, p. 356
Holweger, H., Lemke, M., Rentzsch-Holm, I., Stürenburg, S. 1995, in Nuclei in the Cosmos, AIP Conference Proceedings 327, eds. M. Busso, R. Gallino and C.M. Raiteri, p. 41
Kurucz, R.L. 1970, SAO Special Report No. 309
Kurucz, R.L. 1979, ApJS 40, 1
Kurucz, R.L. 1992, Rev. Mex. Astron. Astrofis., 23, 181
Lemke, M. 1989, A&A 225, 125
Lemke, M. 1990, A&A 240, 331
Michaud, G., Charland, Y., Vauclair, S., Vauclair, G. 1976, ApJ. 210, 447
Rentzsch-Holm, I. 1996, A&A 305, 275
Rentzsch-Holm, I. 1996, A&A 312, 966
Sadakane, K., Okyudo, M. 1989, PASJ 41, 1055 (SO)
Seaton, M.J., Zeippen, C.J., Tully, J.A., Pradhan, A.K., Mendoza, C., Hibbert, A., Berrington, K.A. 1992, Rev. Mex. Astron. Astrofis., 23, 19 (OP)
Steenbock, W., Holweger, H. 1984, A&A 130, 319
Stehlé, C. 1994, A&AS 104, 509
Takada-Hidai, M., Takeda, Y. 1996, PASJ in press (THT)
Vidal, C.R., Cooper, J., Smith, E.W. 1970, J. Quant. Spectrosc. and Rad. Transf. 10, 1011
Vidal, C.R., Cooper, J., Smith, E.W. 1971, J. Quant. Spectrosc. and Rad. Transf. 11, 263
Vidal, C.R., Cooper, J., Smith, E.W. 1973, ApJS 25, 37
Wiese, W.L., Smith, M.W., Glennon, B.M. 1966, Atomic Transition Probabilities Vol. I, Nat. Stand. Ref. Data Ser., Nat Bur. Stand. (U.S.)

This article was processed by the author using Springer-Verlag LaTeX A&A style file *L-AA* version 3.